

# Guanidinylation: A Simple Way to Fabricate Cell Penetrating Peptide Analogue-Modified Chitosan Vector for Enhanced Gene Delivery

Xinyun Zhai,<sup>1</sup> Peng Sun,<sup>1</sup> Yongfeng Luo,<sup>2</sup> Chaonan Ma,<sup>2</sup> Jun Xu,<sup>2</sup> Wenguang Liu<sup>1</sup>

<sup>1</sup>School of Materials Science and Engineering, Tianjin Key Laboratory of Composite and Functional Materials, Tianjin University, Tianjin 300072, China

<sup>2</sup>State Key Laboratory of Respiratory Disease and Guangzhou Institute of Respiratory Disease, Guangzhou Medical College, Guangzhou 510120, Guangdong Province, China

Received 1 November 2010; accepted 10 January 2011

DOI 10.1002/app.34156

Published online 12 April 2011 in Wiley Online Library (wileyonlinelibrary.com).

**ABSTRACT:** In view of the analogous transmembrane function to cell penetrating peptides, guanidine group was incorporated into chitosan by chemical modification to enhance the transfection performance of chitosan vectors. Guanidinylated chitosan (GCS) was shown to be well soluble in neutral aqueous solution. The interaction between GCS with plasmid DNA was characterized by agarose retardation experiment and ethidium bromide displacement assay. GCS formed more stable complexes with DNA under physiological pH than chitosan. The transfection efficiency of GCS was evaluated employing COS-7 cell line—GCS polyplexes demon-

strated higher transfection efficiency and lower cytotoxicity relative to chitosan. The optimum efficiency of GCS was achieved in the vicinity of the critical complexing ratio. The results of flow cytometry indicated that guanidinylation promoted an eightfold increase in the cell uptake. The study revealed that guanidinylated chitosan is a promising candidate as an effective nonviral vector for *in vivo* gene delivery. © 2011 Wiley Periodicals, Inc. *J Appl Polym Sci* 121: 3569–3578, 2011

**Key words:** chitosan; nonviral vector; guanidinylation; cell penetrating peptide

## INTRODUCTION

Nonviral vectors have recently received ever increasing attention due to their potential as an alternative to viral counterparts for gene delivery. Commonly used polymer nonviral vectors include polycations such as chitosan, polyethylenimine (PEI), poly(amido amine) dendrimer and poly(L-lysine). These polymeric carriers were known to have large gene delivery capacities, to be nonimmunogenic and easy to manufacture.<sup>1,2</sup> However, several drawbacks such as cytotoxicity and relatively low transfection efficiency limited their applications.<sup>3</sup>

Cellular uptake, endosomal escape, cytoplasmic mobility, and nuclear entry are deemed to be the

four main barriers for polymer-mediated transfection *in vitro*.<sup>4</sup> Among these barriers, poor uptake of cell or nucleus is the major obstacle encountered by nonviral vector during transfection, and hence needs to be overcome for the development of efficient gene delivery systems.

The poor cellular internalization of nonviral vectors may be due to that the cell membrane only allows foreign molecules meeting specific criteria for size, charge, or chemical composition to enter the cell. Harnessing the transporters embedded in the membrane seems to be an ideal method to solve this problem.<sup>5</sup> Thereby, taking advantage of the nonspecific uptake mechanisms, such as the application of cell penetrating peptides, seems a promising way to break through the cell membrane to deliver nucleic acid.<sup>6</sup> Cell penetrating peptides (CPPs), especially arginine-rich peptides such as HIV-1 Tat, oligoarginine peptides, have been demonstrated to possess the ability to translocate the membrane.<sup>7–9</sup> These peptides such as Tat sequence or Antennapedia homeodomain have received intense interest in drug and gene delivery field due to their efficient translocation of nonpermeant molecules into cells.<sup>10–12</sup> The guanidinium group of CPPs has been suggested to play a key role in the cellular uptake because of its highly basic nature and a specific bidentate hydrogen-bonding formation with the cell membrane.<sup>13,14</sup> Several

Correspondence to: W. Liu (wgliu@tju.edu.cn).

Contract grant sponsor: National Natural Science Foundation of China; contract grant numbers: 30770587, 50973082.

Contract grant sponsor: High Tech Research and Development; contract grant number: 863.

Contract grant sponsor: Programme of China; contract grant number: 2007AA022002.

Contract grant sponsor: Tianjin Municipal Natural Science Foundation; contract grant number: 10JCZDJC17400.

*Journal of Applied Polymer Science*, Vol. 121, 3569–3578 (2011)  
© 2011 Wiley Periodicals, Inc.

works reported that guanidinylation of polymeric vectors could lead to the improved transfection efficiency, meaning simple chemical modification such as guanidinylation can mimic the *trans*-membrane activity of CPPs facilitating nanoparticles into cells.<sup>15–17</sup>

Of the polymers utilized as nonviral vectors, chitosan, comprised of  $\beta$ -(1-4) linked 2-amino-2-deoxy-D-glucose, has been proposed as one of the potential nonviral vectors for gene transfer,<sup>18</sup> benefiting from its cationic character, biodegradability, and biocompatibility. However, the practical use of chitosan is limited by the low transfection efficiency and insolubility in water.<sup>19</sup> To improve transfection efficiency of chitosan polyplexes, numerous modification strategies have been exploited in the past decades.<sup>20</sup> Introducing arginine-rich peptides or NLS peptide to chitosan has already shown to promote the uptake of cell or nucleus and hence enhance the transfection efficiency of chitosan ultimately.<sup>21</sup> However, the application of peptides mentioned above is potentially fraught with a number of scientific and technical problems, which include instability by endogenous peptidases, uncertain *in vivo* delivery efficiency, as well as potential toxicity and immunogenicity liabilities.<sup>6</sup>

In this study, based on the central role played by guanidinium group in the cellular transport, we will modify the primary amine groups of chitosan with guanidine groups, intending to not only enhance the cellular uptake of vectors, but also avoid the potential problems with the application of peptides. We will investigate the physiochemical properties, cytotoxicity and transfection efficiency of guanidinylated chitosan (GCS)/DNA complexes. Additionally, we will examine the cellular uptake profile of GCS/DNA polyplexes.

## EXPERIMENTAL

### Materials

Chitosan (CS, molecular weight 50 kDa, deacetylation degree 83%) was supplied by AK Biotech (Shandong, China). Cyanamide (98%) was purchased from Alfa Aesar Chemical (Tianjin, China). Branched polyethyleneimine (PEI25K, 25 kDa), ethidium bromide (EB, 95%), and 3-(4,5-dimethylthiazol-2-yl)-2,5-diphenyl tetrazoliumbromide (MTT, 98%) were supplied by  $\zeta$ -Aldrich (Shanghai, China). Plasmid pGL3-control with SV40 promoter and enhancer sequences encoding luciferase was obtained from Promega, Madison, WI. pEGFP-C1 encoding a red-shifted variant of wild-type green fluorescent protein (GFP) was provided by Clontech, Mountain View, CA. The plasmids were amplified in *Escherichia coli* and puri-

fied by the differential precipitation method. All other reagents used were of analytical grade.

### Synthesis of guanidinylated chitosan

Guanidinylated chitosan (GCS) was prepared according to the method given in the literature. Briefly, chitosan (CS, 0.32 g) was added into a hydrochloric acid solution (0.33M, 30 mL). Then an appropriate amount of cyanamide was added and the resulting solution was kept at 90°C under stirring for 12 h. Finally, the mixture was dialyzed against water (MWCO of 3500) for 5 days and lyophilized. Herein, two substitution degrees of GCSs were synthesized by using different amounts of cyanamide, that is, molar ratios of cyanamide to chitosan primary amino, 2 : 1, 4 : 1; the resultant derivatives were denoted as GCS1 and GCS2, respectively.

### Characterization of GCS

FTIR spectra of CS and GCS2 were recorded over wavenumber range of 4000–500  $\text{cm}^{-1}$  on an ATR-FTIR spectrophotometer (Perkin-Elmer spectrum 100, USA). <sup>13</sup>C NMR spectra of CS and GCS2 were measured with a UNITY plus-500 NMR spectrometer (Varian, USA) using  $\text{DCl}/\text{D}_2\text{O}$  and  $\text{D}_2\text{O}$ , respectively. The degree of substitution was determined by elemental analysis (C, N, H) of samples (ELEMENTAR Vario EL, Germany).

### Preparation of GCS/DNA complexes

CS was dissolved in acetic acid/sodium acetate buffer (0.1M, pH = 5.0); while GCS1 and GCS2 were dissolved in distilled water to form diluted solutions. The solutions were sterilized by passage through 0.22- $\mu\text{m}$  filter prior to complexation. Polymer/pDNA complexes at different weight ratios were formulated by adding filtered polymer solutions of prescribed concentrations to an equal volume of a defined pDNA solution, vortexed for 15 s, and then incubated for 30 min at room temperature.

### Gel retardation assay

The polymer/pDNA complexes at different weight ratios were prepared freshly as described above. The formed complex solutions (5  $\mu\text{L}$ ) were mixed with a loading buffer, and then loaded into 1% agarose gel containing ethidium bromide (0.5  $\mu\text{g mL}^{-1}$ ). Gel electrophoresis was run at room temperature in TAE buffer at 100 V for 30 min.

### Ethidium bromide displacement

Ethidium bromide (EB) ( $10 \text{ mg mL}^{-1}$ ) was mixed with DNA solution at a weight ratio of 1 : 6 (EB-DNA) to prepare EB-DNA solution. Complexes were formed by adding different polymer solutions of a desired concentration to equal volumes of EB/DNA solution. After incubation for 30 min, the polymer/EB/DNA solutions were diluted with PBS buffers of different pH values (from 4 to 8), and placed at room temperature for another 30 min. Steady-state fluorescence measurement was performed on a Synergy HT Spectrofluorometer at an excitation wavelength of 530 nm and an emission wavelength of 590 nm. Relative fluorescence values of polymer/EB-DNA solutions were calculated by using  $[(F_C - F_I)/(F_D - F_I)] \times 100\%$ , where  $F_I$ ,  $F_D$ , and  $F_C$  are fluorescence of free EB, EB-DNA, and EB-DNA after each addition of polymer. Triplicate samples were used for each measurement.

### Transmission electron microscopy (TEM)

The morphology and size of polymer/pDNA complexes with different ratios were observed using TEM (JEOL JEM-100CXII). Briefly, polymer/pDNA complexes were formed to a concentration of  $10 \text{ mg mL}^{-1}$ . A drop of the complex solution was deposited on a carbon-coated grid. After 5 min, 1.5 wt % phosphotungstic acid (PTA) was added to negatively stain the complexes, and then the complexes were recorded on films with TEM.

### Measurement of particle size and $\zeta$ -potential

The particle sizes and  $\zeta$ -potentials of polymer/pDNA complexes were measured using a Zeta-PALS/Zeta Potential Analyzer (Brookhaven, Austria) at  $25^\circ\text{C}$ . The complexes were prepared by adding an appropriate volume of polymer solution to  $1 \mu\text{g}$  of DNA solution at weight ratios ranging from 0.5 to 5. Then the solutions containing complexes were diluted by distilled water to 3 mL for particle size and  $\zeta$ -potential measurement.

### Cell culture

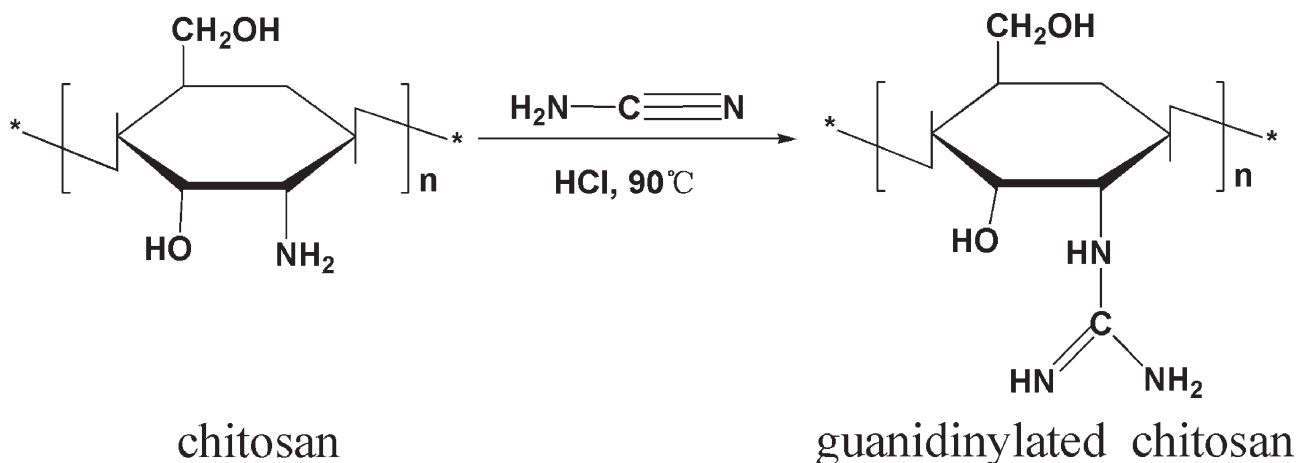
African green monkey kidney cells (COS-7) and Human embryonic kidney cells (HEK293) were purchased from Peking Union Medical College (Beijing, China). Both the cells were grown in the essential medium DMEM supplemented with 10% fetal calf serum at  $37^\circ\text{C}$  in a 5%  $\text{CO}_2$  humidified air atmosphere.

### Cytotoxicity assay

The cytotoxicity of CS, GCS1, and GCS2 were evaluated by MTT assay using COS-7 cells. Briefly,  $5 \times 10^4$  cells/well were seeded in 96-well plates and incubated for 24 h at  $37^\circ\text{C}$  in 5%  $\text{CO}_2$  humidified atmosphere. Polymers at an increasing concentration from 0 to  $400 \mu\text{g mL}^{-1}$  was added to each well and incubated for 24 h before refreshing the medium with fresh complete medium ( $200 \mu\text{L well}^{-1}$ ). After additional incubation for 24 h,  $20 \mu\text{L well}^{-1}$  MTT ( $5 \text{ mg mL}^{-1}$  in PBS) was added to each well, and the plate was further incubated for 4 h. Then all media were removed and  $150 \mu\text{L well}^{-1}$  DMSO was added. The plate was gently shaken for 10 min. The absorbance of each well was measured at 570 nm on a  $\Sigma 960$  plate-reader (Metertech) with pure DMSO as a blank. Nontreated cells were used as a control and the relative cell viability (mean%  $\pm$  SD,  $n = 3$ ) was expressed as  $\text{Abs}_{\text{sample}}/\text{Abs}_{\text{control}} \times 100\%$ .

### *In vitro* transfection

COS-7 cells were seeded at a density of  $2 \times 10^5$  cells/well in 24-well plates and incubated for 24 h at  $37^\circ\text{C}$  in 5%  $\text{CO}_2$  humidified atmosphere. Prior to transfection the culture medium was removed and replaced with DMEM supplemented with 10% FBS without antibiotics ( $450 \mu\text{L well}^{-1}$ ). Various complexes at different weight ratios were formed based on the aforementioned protocol and added to the 24-well plates ( $50 \mu\text{L}$  in water, containing  $1 \mu\text{g DNA/well}$ ). After incubating at  $37^\circ\text{C}$  in 5%  $\text{CO}_2$  for 24 h, the medium containing complex solution was then replaced with  $500 \mu\text{L}$  of fresh complete medium and the cells were incubated for an additional 24 h. Transfection tests were performed in triplicate. Following incubation, the medium was removed, and the cells were washed with PBS twice. The cells in each well were treated with  $150 \mu\text{L}$  of reporter lysis buffer (RLB, Promega) followed by freeze-thaw cycles to ensure complete lysis. The lysate was centrifuged for 4 min at  $13,000 \times r \text{ min}^{-1}$  at room temperature and the supernatant was collected for luminescence measurements. The luminescence of each sample was measured by 1420 Multilabel counter (Wallac, USA) using Bright-Glo™ luciferase assay system (Promega, USA) according to the manufacturer's protocol. The results were expressed as relative light units (RLU) per milligram of cell protein, and the protein concentration of each well was measured by a BCA protein assay (Pierce, Rockford, IL). The 25 kDa branched polyethylenimine (PEI) was used as a positive control. PEI/DNA complexes were prepared at a 2/1 mass ratio of PEI to DNA.



Scheme 1 Synthesis of guanidinylated chitosan.

### Measurement of cellular internalization

pGL-3 plasmid was labeled with YOYO-1 dye as follows: 1 mM YOYO-1 was diluted 1 : 100 in PBS. Then 10  $\mu\text{g}$  of pDNA was mixed with 10  $\mu\text{L}$  YOYO-1 dilution (1 molecule of YOYO-1 per 152 base pairs of pDNA) and incubated for 2 h in the dark.

YOYO-1 Labeled-pDNA was used to form CS/DNA and GCS/DNA complexes under an optimum weight ratio. HEK293 cells were seeded in six-well plates ( $8 \times 10^5$  cells per well) overnight and the medium was replaced with DMEM plus 10% FBS without antibiotics. Complexes were added in the plate (4  $\mu\text{g}$  pDNA per well) and incubated for desired hours. For flow cytometry study, complexes were aspirated off and the cells were washed with cold PBS, trypsinized by trypsin-EDTA, and harvested in PBS. Fluorescence intensity and distribution of the cells were measured by flow cytometry (Epics Altra, Beckman Coulter). The distribution of internalized labeled DNA complexes was visualized under a laser confocal microscope (Nikon, model number Japan).

## RESULTS AND DISCUSSION

### Characterization of guanidinylated chitosan

The conversion of amines to guanidine by cyanamide in acidic medium at an elevated temperature, is a general method for preparing guanidine derivatives.<sup>22</sup> By this means, the synthesis of the guanidinylated chitosan was achieved by one step procedure as shown in Scheme 1.

The formation of guanidinylated chitosan can be confirmed by FT-IR spectra (Fig. 1). Compared with chitosan, GCS2 shows new stronger peaks at 1652 and 1550  $\text{cm}^{-1}$  assigned to the stretching vibration of C=N and distortion vibration of N-H, respectively. The new band at 1374  $\text{cm}^{-1}$  is attributed to

the stretching vibration of C-N-C. The results suggest that amino groups of chitosan have been converted into guanidinium.<sup>23</sup>

In the  $^{13}\text{C}$  NMR spectra of CS and GCS2 (Fig. 2), the feature bands of chitosan at 56.5(C2), 60.8(C6), 70.6(C3), 75.3(C5), 77.5(C4), 98.0(C1) (ppm) are clearly shown. For GCS2, a new signal located at 158.43 ppm is assigned to the carbon of guanidine group,<sup>24</sup> which further confirms the successful introduction of guanidinium group to chitosan. It is noted that GCS becomes highly water soluble because the introduced guanidinium groups are highly basic and positively charged over a wide pH range.

The degrees of substitution for GCS1 and GCS2 were estimated through elemental analysis. The data of elemental analysis are listed in Table I. Based on the C/N wt % in CS, GCS1, and GCS2, the degrees of substitution of guanidine group, expressed as the number of guanidinium groups per 100 anhydroglucose units of chitosan, can be calculated. In this

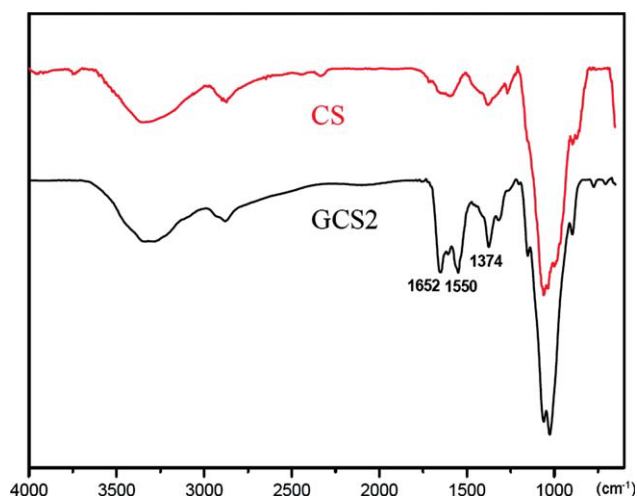


Figure 1 FT-IR spectra of chitosan (CS) and guanidinylated chitosan (GCS). [Color figure can be viewed in the online issue, which is available at [wileyonlinelibrary.com](http://www.interscience.wiley.com).]



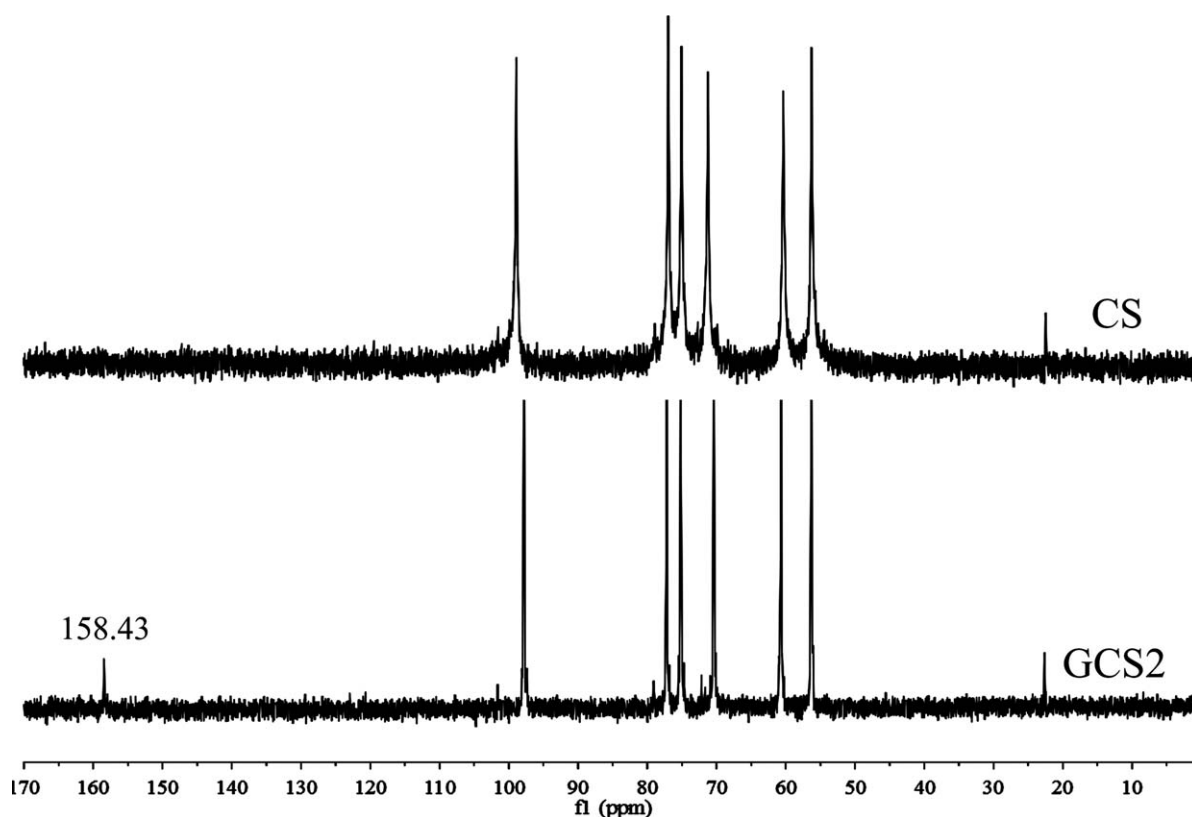


Figure 2  $^{13}\text{C}$  NMR spectra of chitosan (CS) and guanidinylated chitosan (GCS2).

experiment, though a large excess of cyanamide was used for guanidinylation, only 8.5 and 14.2% substitution degrees were achieved. A possible reason is that hydrolysis side reaction of cyanamide occurred during the guanidinylation reaction.<sup>25</sup>

### Characterization of polyplexes

To investigate the DNA condensation capacity of guanidinylated chitosan, gel retardation assay of polyplexes was conducted. As presented in Figure 3, CS/DNA and GCS/DNA complexes were prepared at various weight ratios ranging from 0.1 : 1 to 4 : 1. It is seen that the critical complexing ratios of CS, GCS1, and GCS2 are 0.75, 1, and 2, respectively. This indicates that both chitosan and guanidinylated chitosan are capable of condensing DNA efficiently at low ratio. On the other hand, the critical complexing ratio increases as the content of guanidine group is augmented, manifesting guanidinylated chitosan exhibits a weaker binding strength with DNA compared to chitosan. That is because apart from strong electrostatic interaction, part of guanidine groups may form hydrogen bonding interactions with DNA,<sup>26</sup> and this weaker attraction force inevitably reduces the binding ability of GCS with DNA than amines as reported previously.<sup>16</sup>

It is well documented that chitosan becomes soluble and can form polyelectrolyte complexes with polyanions as pH is below its pKa, 6.5.<sup>27</sup> While at higher pH (pH > 6.5), chitosan starts to be deprotonated, which leads to the reduction in the ability to bind DNA.<sup>28</sup> Since gene transfection experiments are often conducted under physiological pH, that could greatly restrict the use of chitosan vector in clinical trials. In comparison to amino group, guanidine groups remain protonated under a wide range of pHs due to its highly basic character (pKa = 12.5).<sup>13</sup> Additionally, guanidine derivatives can generate a complementary guanidinium-phosphate interaction with DNA, which can contribute to the formation of stable complexes.<sup>17</sup> The results of EB-displacement with addition of CS or GCS at a fixed ratio of 2 : 1 under different pH values are shown in Figure 4. At the same pH, the fluorescence intensity of EB-DNA/GCS is lower than that of chitosan system. This

TABLE I  
Results of Elemental Analysis and Substitution Degree

Sample	Analysis found (Calc.) %				
	C	N	H	C/N	DS%
CS	40.82	7.28	7.21	6.54	–
GCS1	36.78	6.89	6.93	6.23	8.4
GCS2	37.13	7.19	6.90	6.02	14.2

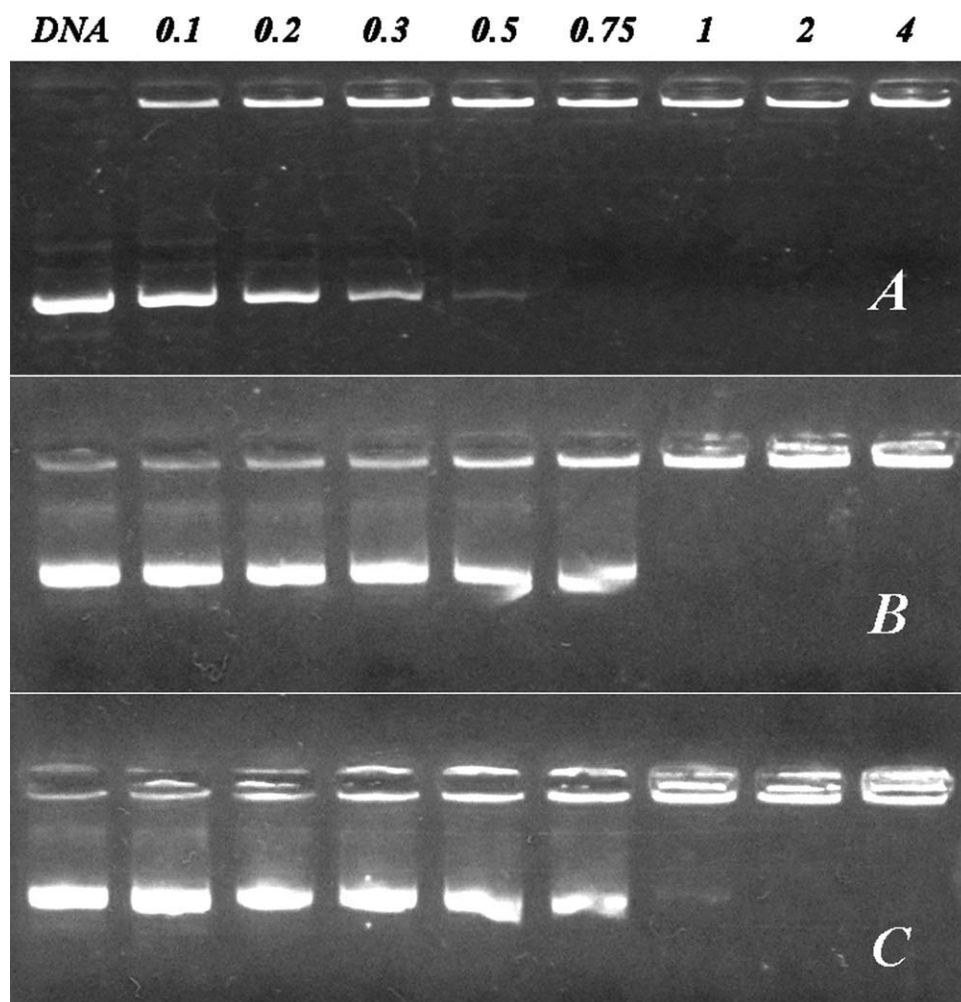


**Figure 3** Agarose gel electrophoresis of CS/DNA (A), GCS1/DNA (B) and GCS2/DNA (C) complexes. Numbers above the lane represent the weight ratios of complexes (polymer : DNA).

implies that at a ratio of 2 : 1, GCS condenses DNA to a more compact state than CS due to additional hydrogen bonding interaction between guanine and phosphate groups of DNA. This non-electrostatic interaction cannot be detected by retardation DNA bands on electrophoresis because H-bonding does not neutralize the negative charges. At the neutral pH and physiological pH, the guanidylated chitosans (GCS1 and GCS2) maintain a relative stronger DNA-binding ability in spite of occurrence of slight increase in fluorescence intensity. Comparatively, the relative fluorescence intensity of EB-DNA after adding chitosan at pH 7.4 goes up to above 70%, evidencing the DNA condensation capability of chitosan is seriously weakened. In this case, most DNA molecules are unpacked from chitosan. The higher stability of GCS/DNA under physiological pH portends its promising potential application in mediating gene transfection *in vivo*.

TEM was used to examine the morphology of the complexes formed at weight ratios of 1 : 1, 2 : 1, and

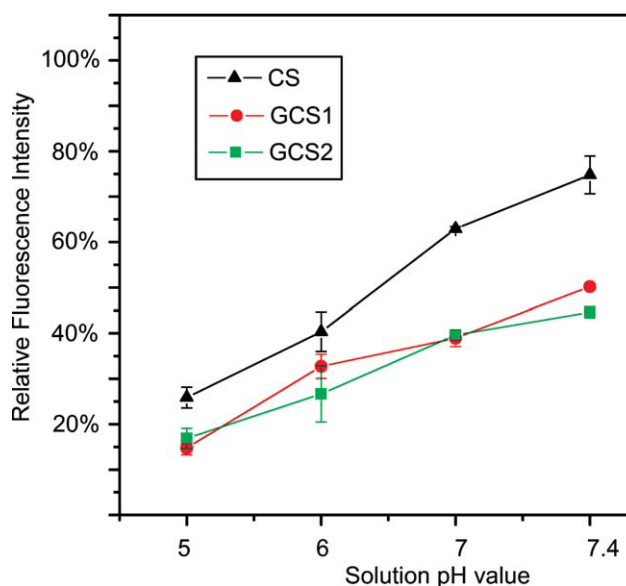


**Figure 4** EB-DNA displacement by CS, GCS1 and GCS2 at a weight ratio of 2 under different pH values. [Color figure can be viewed in the online issue, which is available at [wileyonlinelibrary.com](http://wileyonlinelibrary.com).]

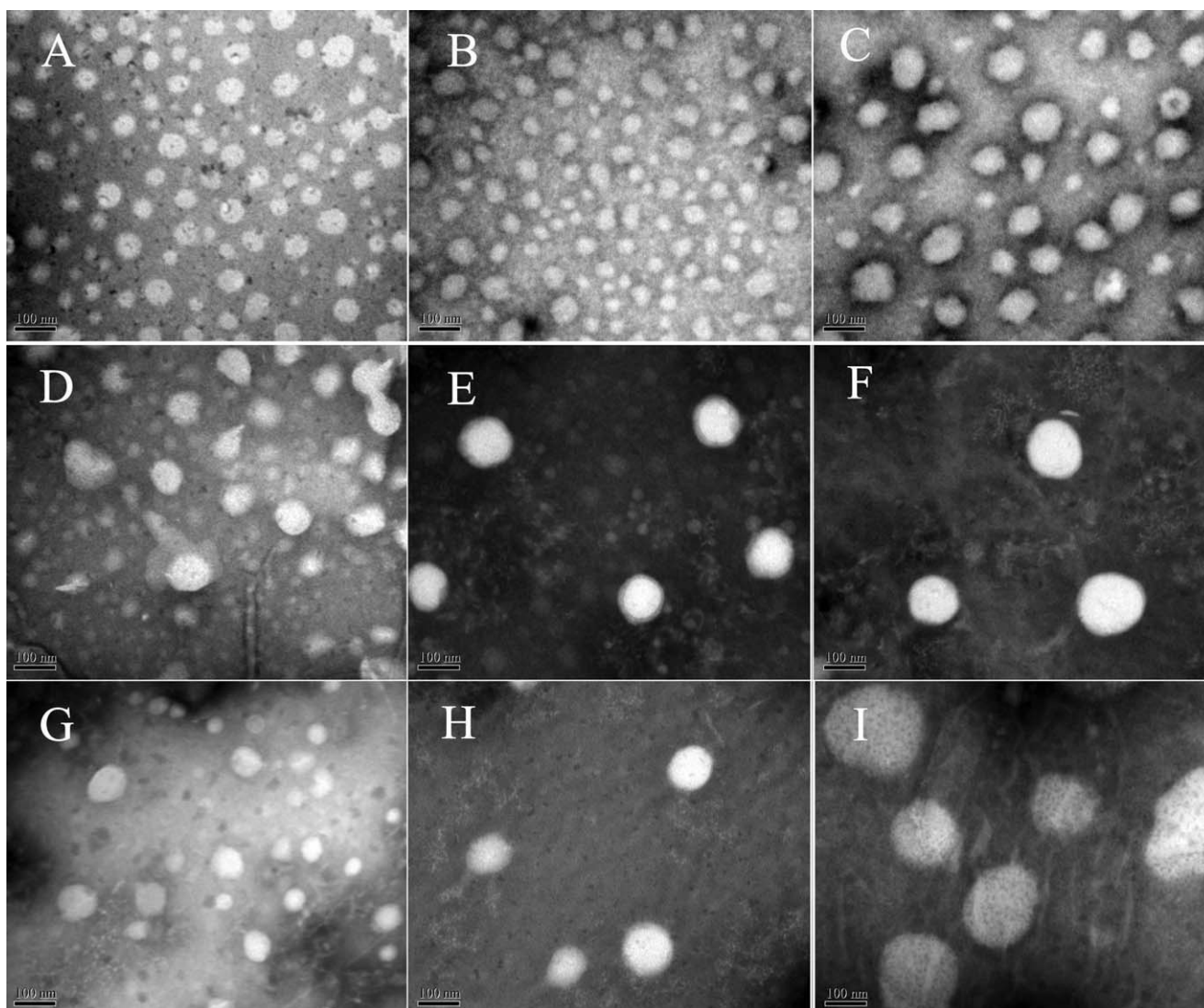


**Figure 5** TEM images of polymer/DNA complexes at different weight ratios. CS/pDNA: (A) 1 : 1, (B) 2 : 1, (C) 5 : 1; GCS1/pDNA: (D) 1 : 1, (E) 2 : 1, (F) 5 : 1; GCS2/pDNA: (G) 1 : 1, (H) 2 : 1, (I) 5 : 1.

5 : 1. As shown in Figure 5, all the polymers condense DNA into spherical nanosized particles with diameters ranging from 50 to 200 nm. The particle sizes of the three polyplexes increase along with an increment in weight ratio. This may be attributed to the occurrence of complex aggregation while the complexing ratio is above a critical value.

It is noted that guanidinylated chitosan/DNA complexes show much larger size at a high weight ratio (5 : 1) compared with chitosan/DNA complexes.

The particle sizes of the complexes measured with a ZetaPALS/Zeta Potential Analyzer are tabulated in Table II. With the weight ratio increasing from 0.5 : 1 to 5 : 1, the particle sizes of CS/DNA

**TABLE II**  
Particle Sizes of CS/DNA, GCS1/DNA, and GCS2/DNA Polyplexes at Different Weight Ratios

Vector/DNA (w/w)	Particle size (nm)		
	CS	GCS1	GCS2
0.5 : 1	244.3 ± 4.2	597.3 ± 14.1	545.5 ± 15.9
1 : 1	343.2 ± 5.7	470.3 ± 15.0	396.1 ± 14.8
2 : 1	462.0 ± 13.8	598 ± 5.9	572.6 ± 8.6
5 : 1	460.1 ± 25.0	797.4 ± 44.1	845.0 ± 17.8



**TABLE III**  
Zeta Potentials of CS/DNA, GCS1/DNA, and GCS2/DNA Polyplexes at Different Weight Ratios

Vector/DNA (w/w)	Zeta potential (mV)		
	CS/DNA	GCS1/DNA	GCS2/DNA
0.5 : 1	7.02 ± 1.1	-2.79 ± 0.85	-4.10 ± 2.1
1 : 1	13.2 ± 0.5	6.59 ± 1.5	3.78 ± 1.8
2 : 1	15.5 ± 0.2	10.5 ± 0.8	8.03 ± 0.6
5 : 1	17.4 ± 4.18	13.8 ± 0.5	10.2 ± 1.5

complexes exhibits a rising trend; while the diameters of GCS1/DNA and GCS2/DNA complexes show a minimum value at 1 : 1. At the weight ratio of 5 : 1, the particle sizes of GCS/DNA are much larger than that of CS/DNA complexes, which is similar with the above TEM observation. This phenomena may be due to the self-aggregation of GCS complexes caused by hydrogen bonding interaction between the guanidine groups at a higher complexing ratio.<sup>29</sup> The larger size observed with laser particle size analyzer relative to TEM is due to the hydration of nanoparticles in solution.

From Table III, we can see that GCS1 and GCS2 complexes show lower surface charges than CS complexes. The decreased surface charge is mainly due to the hydrogen bonding interaction of guanidinium with phosphate of DNA. This nonelectrostatic interaction does not cause charge neutralization. The decreased surface charge tends to reduce the electrostatic repulsion between GCS/DNA complex nanoparticles, thereby leading to the aggregation of particles.

### Cytotoxicity assay

To assay the influence of guanidinylation on cytotoxicity, we evaluated the relative cell viability of CS,

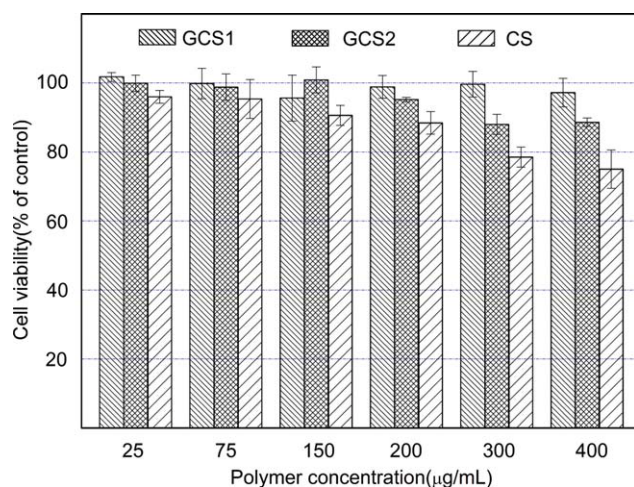


**Figure 6** Viability of COS-7 cells versus the concentrations of CS, GCS1, and GCS2.

GCS1, and GCS2 at various concentrations by MTT assay method. It is evident from Figure 6 that all the three vectors exhibit concentration dependent cytotoxicity. At a concentration of 200  $\mu\text{g mL}^{-1}$ , the cell viability of all three groups maintains above 80%. At the same concentration of GCS, more than 90% cells remains viable. The relatively higher cytotoxicity of chitosan is mainly due to the acetic acid included to dissolve chitosan. The MTT results prove that the guanidynylated chitosan is a low cytotoxic vector for gene delivery.

### In vitro transfection

Transfection experiments were performed in COS-7 cells using the pGL-3 luciferase plasmid. CS, GCS1, and GCS2 polyplexes were prepared at different weight ratios from 0.5 to 5 (Fig. 7). Over the selected range of complexing ratio, GCSs show higher efficiency relative to CS at the same vector/DNA ratio, indicating that guanidinylation indeed promotes the transfection efficiency of chitosan vectors. In comparison, the transfection level of GCS2 is generally higher than that of GCS1 at the identical complexing ratio. A plausible reason is that for GCS2, higher content of guanidine groups lead to the increased

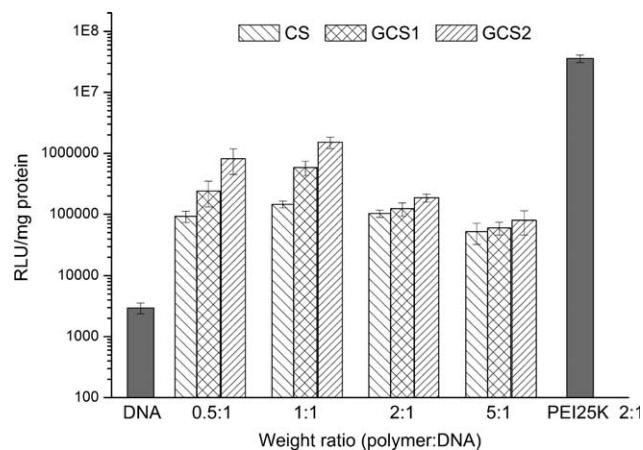


**Figure 7** In vitro transfection efficiency of CS/DNA, GCS1/DNA, and GCS2/DNA complexes at various weight ratios evaluated with luciferase activity in COS-7 cell line (mean ± SD,  $n = 3$ ).



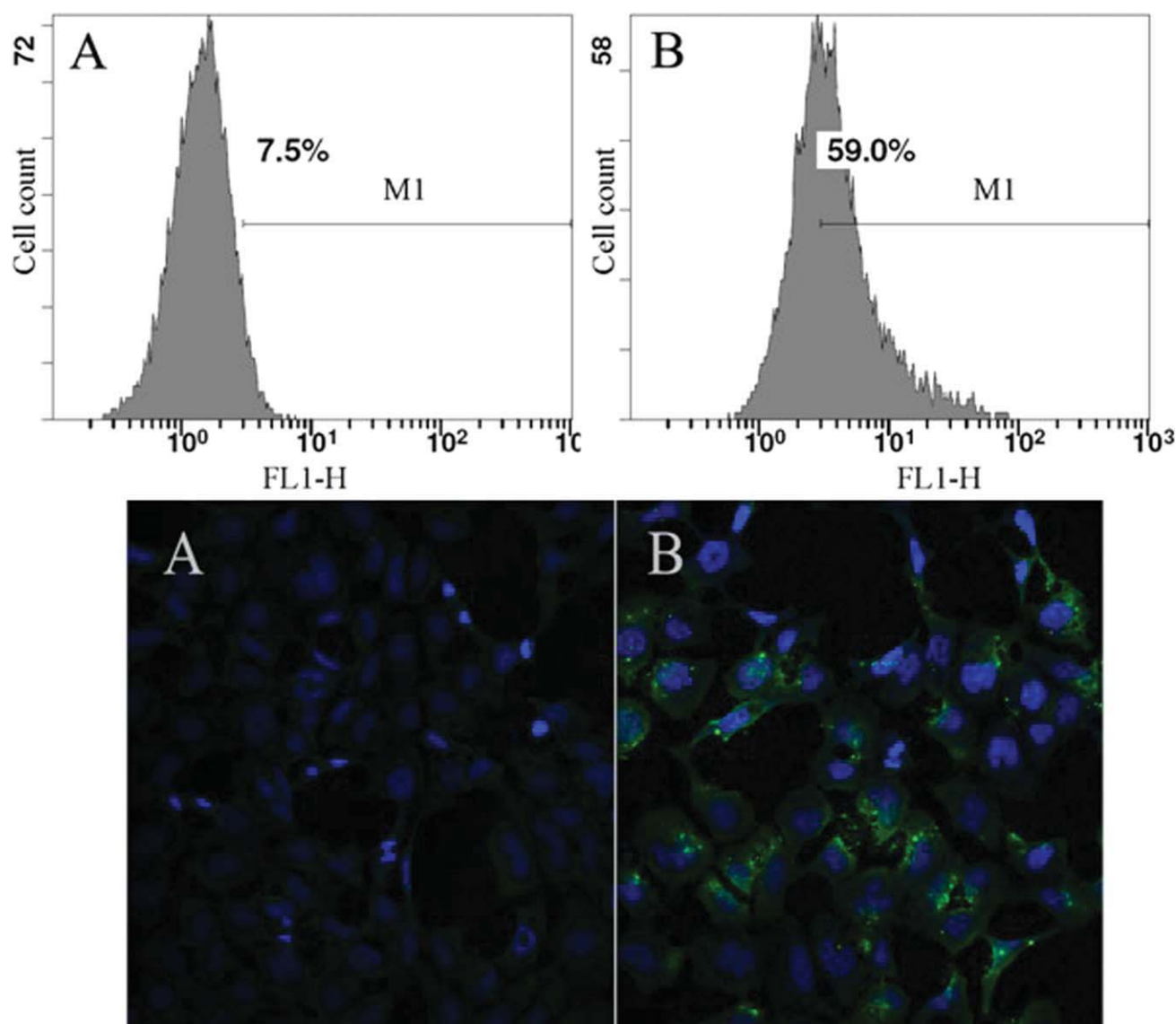


**Figure 8** Cellular uptake of complexes assayed by flow cytometry and intracellular trafficking into HEK293 cells observed by confocal microscopy. (magnification:  $\times 100$ ). (A: CS/pDNA; B: GCS2/pDNA, at the weight ratio of 1 : 1). [Color figure can be viewed in the online issue, which is available at [wileyonlinelibrary.com](http://wileyonlinelibrary.com).]

cellular uptake of polyplexes. Noteworthy, in the vicinity of critical complexing ratio, the higher transfection level is achieved. The transfection efficiency of GCS2 is sevenfold higher than that of unmodified chitosan at a ratio of 1 : 1, which is slightly lower than the critical complexing ratio, 2 : 1. We thought that the specific bidentate hydrogen-bondings formed between guanidine and cell membrane aid in the translocation of complexes. Another phenomenon is that as the complexing ratio is above 1 : 1, the transfection efficiency starts to decline. An explanation is that as the ratios exceed critical value, nanocomplexes aggregate into larger assemblies, thus decreasing the cellular uptake; on the other hand, excessive vector may hinder the unpacking of condensed DNA. All these factors contribute to lower transfection level. It is noted that the transfec-

tion ability of guanidynylated chitosan is still significantly inferior to that of PEI25K (Fig. 7). Guanidinylation of varied molecular weight chitosans as well as tuning substitution degree to optimize transfection efficiency is underway in our lab.

#### Cellular uptake of polyplexes

To investigate the effect of guanidine on the increased cellular uptake of polyplexes, we used flow cytometry to measure the amount of DNA internalized by transfected cells. CS and GCS were complexed with YOYO-1-labeled DNA, respectively, and then the cellular uptake of labeled polyplexes was investigated by flow cytometry in HEK293 cells. Each cellular uptake value (%) was calculated by setting up M1 region as a gate. As shown in Figure 8,

the cellular uptake rate of GCS2/DNA polyplexes was estimated to be 59%; while that of CS/DNA polyplexes was only 7.5%. GCS1 presents an uptake value of 27% (figure not shown). Regarding the fact that cellular uptake of polyplexes is one of main barriers for chitosan vectors, the results corroborate that guanidinylation significantly enhances the cellular endocytosis of chitosan-based vectors, thereby contributing to the improvement of transfection efficiency.

From confocal fluorescence microscopy images, we can also directly observe the enhanced cellular uptake of guanidylated chitosan. In Figure 8, although we cannot find the apparent enrichment of GCS/DNA polyplexed in nucleus, most of complex particles are prone to locate around the nucleus (blue regions). Considering the difficulty of cytoplasmic mobility to nucleus, we think that the guanidylated chitosan acts as nuclear localization function, which may play an additional role in enhancing the transfection efficiency.<sup>17</sup>

### CONCLUSIONS

Guanidylated chitosan (GCS) was conveniently prepared by simply converting amines of chitosan into guanidinos. A significant improvement in water-solubility was achieved after guanidinylation. GCS showed a stronger DNA condensation ability under physiological pH than chitosan. Guanidylated chitosan was able to condense DNA to nanoparticles which were dependent upon the complexing ratios. Because of weakening electrostatic interaction as well as no acetic acid use, GCS showed lower cytotoxicity compared to parent chitosan. The transfection efficiency of GCS was superior to that of chitosan at the optimum weight ratio 1 : 1. The cellular uptake rate of GCS2/DNA polyplexes was eightfold higher than that of CS/DNA polyplexes, indicating that guanidinylation significantly enhanced the cellular endocytosis of chitosan-based vectors.

### References

- Liu, F.; Huang, L. *J Controlled Release* 2002, 78, 259.
- Luo, D.; Saltzman, W. M. *Nat Biotechnol* 2000, 18, 33.
- Wong, S. Y.; Pelet, J. M.; Putnam, D. *Prog Polym Sci* 2007, 32, 799.
- Mintzer, M. A.; Simanek, E. E. *Chem Rev* 2009, 109, 259.
- Alper, J. *Science* 2002, 296, 838.
- Chung, S. K.; Maiti, K. K.; Lee, W. S. *Int J Pharm* 2008, 35, 16.
- Melikov, K.; Chernomordik, L. V. *Cell Mol Life Sci* 2005, 62, 2739.
- Futaki, S. *Biopolymers* 2006, 84, 241.
- Yamanouchi, D.; Wu, J.; Lazar, A. N.; Kent, K. C.; Chu, C. C.; Liu, B. *Biomaterials* 2008, 29, 3269.
- Fuchs, S. M.; Raines, R. T. *ACS Chem Biol* 2007, 2, 167.
- Kim, T. I.; Baek, J. U.; Yoon, J. K.; Choi, J. S.; Kim, K.; Park, J. S. *Bioconjug Chem* 2007, 18, 309.
- Cryan, S. A.; Devocelle, M.; Moran, P. J.; Hickey, A. J.; Kelly, J. G. *Mol Pharm* 2006, 3, 104.
- Wender, P. A.; Galliher, W. C.; Goun, E. A.; Jones, L. R.; Pillow, T. H. *Adv Drug Deliv Rev* 2008, 60, 452.
- Sakai, N.; Matile, S. *J Am Chem Soc* 2003, 125, 14348.
- Bromberg, L.; Raduyk, S.; Hatton, T. A.; Concheiro, A.; Rodriguez-Valencia, C.; Silva, M.; Alvarez-Lorenzo, C. *Bioconjug Chem* 2009, 20, 1044.
- Zhang, B. Q.; Ji, W. H.; Liu, W. G.; Yao, K. D. *Int J Pharm* 2007, 331, 116.
- Kim, T. I.; Lee, M.; Kim, S. W. *Biomaterials* 2010, 31, 1798.
- Lee, K. Y.; Kwon, I. C.; Kim, Y. H.; Jo, W. H.; Jeong, S. Y. *J Controlled Release* 1998, 51, 213.
- Kim, T. H.; Jiang, H. L.; Jere, D.; Park, I. K.; Cho, M. H.; Nah, J. W.; Choi, Y. J.; Akaike, T.; Cho, C. S. *Prog Polym Sci* 2007, 32, 726.
- Chang, K. L.; Higuchi, Y.; Kawakami, S.; Yamashita, F.; Hashida, M. *Bioconjug Chem* 2010, 21, 1087.
- Opanasopit, P.; Rojanarata, T.; Apirakaramwong, A.; Ngawhirunpat, T.; Ruktanonchai, U. *Int J Pharm* 2009, 382, 291.
- Bernatowicz, M. S.; Wu, Y. L.; Matsueda, G. R. *J Org Chem* 1992, 57, 2497.
- Hu, Y.; Du, Y. M.; Yang, J. H.; Kennedy, J. F.; Wang, X. H.; Wang, L. S. *Carbohydr Polym* 2007, 67, 66.
- Brzozowski, Z.; Saczewski, F.; Gdaniec, M. *Eur J Med Chem* 2002, 37, 285.
- Tordini, F.; Bencini, A.; Bruschi, M.; de Gioia, L.; Zampella, G.; Fantucci, P. *J Phys Chem A* 2003, 107, 1188.
- Ohara, K.; Smietana, M.; Restouin, A.; Mollard, S.; Borg, J. P.; Collette, Y.; Vasseur, J. J. *J Med Chem* 2007, 50, 6465.
- Dai, H.; Jiang, X.; Tan, G. C.; Chen, Y.; Torbenson, M.; Leong, K. W.; Mao, H. Q. *Int J Nanomed* 2006, 4, 507.
- Strand, S. P.; Danielsen, S.; Christensen, B. E.; Vårum, K. M. *Biomacromolecules* 2005, 6, 3357.
- Miyake, M.; Oyama, N. *J Colloid Interface Sci* 2009, 330, 180.